Synthesis in Pure Ethanol and Characterization of Nanosized Calcium Phosphate Fluoroapatite

Pierre Layrolle* and Albert Lebugle

Laboratoire des Matériaux—Physico-chimie des Solides, URA CNRS 445, Ecole Nationale Supérieure de Chimie, Institut National Polytechnique de Toulouse, 38 rue des 36 ponts, 31400 Toulouse Cedex, France

Received July 1, 1995. Revised Manuscript Received October 16, 1995[⊗]

A fluoridated calcium phosphate CPF powder was synthesized in anhydrous ethanol starting from $Ca(OEt)_2$, H_3PO_4, and NH_4F reagents. Two other materials, CP and CF, were also obtained without, respectively, the fluoride and the phosphate source to understand the mechanism of formation of the CPF solid. The vacuum-dried precipitate CF was fully crystallized and identified as calcium fluoride CaF_2. In contrast, the vacuum-dried precipitates CPF and CP, which have Ca/P ratios close to 1.67, were amorphous to XRD. The amorphous sample CPF had the same chemical composition as that of a fluoroapatite $Ca_{10}(PO_4)_6F_2$ compound. The XPS spectroscopy showed that this amorphous solid CPF was homogeneous and was not a mixture of $Ca_9(PO_4)_6$ and CaF_2 phases. The thermal behavior was studied by TGA, DTA, XRD, SEM, and IR spectroscopy. The analyses confirmed the homogeneity of the amorphous CPF precipitate, which crystallized, at 460 °C into a pure fluoroapatite phase. The starting nanosized CPF powder has shown its high reactivity with a very active sintering at 500 °C.

Introduction

Apatitic calcium phosphate is a large family of isostructural compounds derived from the ideal hydroxyapatite [$Ca_{10}(PO_4)_6(OH)_2$; HAP] in which many substitutions can occur.[1] Apatites have numerous industrial applications in different fields, for example, as gas sensors, ionic conductors, laser hosts, catalysts, and chromatographic adsorbers.[2] Moreover, they have attracted much interest as substitute biomaterials for damaged bone and teeth over the past several decades due to their chemical and crystallographical similarities to the inorganic matrix of the hard tissues in vertebrates.[3,4] As synthetic HAP has good biocompatibility and bioactivity but poor mechanical properties, this material has been widely used in the form of ceramics, films, and plasma spray coating of metal prostheses for implants in medicine and dentistry.[5−9]

Hydroxyapatite easily forms solid solutions with fluoroapatite [$Ca_{10}(PO_4)_6F_2$; FAP] because these two compounds are crystallized in a hexagonal system and their lattice parameters are similar.[10,11] Hydroxyl- and fluoroapatite are also characterized by the presence of channels parallel to the *c* axis where HO^- and F^- ions (two for each unit cell) are localized.[12] The solid solutions between HAP and FAP, named fluorohydroxyapatite [$Ca_{10}(PO_4)_6F_{2x}(OH)_{2-2x}$; FHAP], have been widely studied because of their biological importance in the disease of dental caries.[13−16] It has been established by IR and NMR spectroscopies[17,18] that FHAP is stabilized by a hydrogen bond between hydroxide and fluorine ions which forms −O−H−F− chains along the channel of the apatitic structure. Therefore, the FHAP solid solutions show very high thermodynamic stability and very low solubility in water.[13,15]

The synthesis methods of the end member of the FHAP solid solutions, the stoichiometric fluoroapatite (F content: 3.77 wt %, $x = 1$), have been extensively investigated.[19−21] For example, FAP can be prepared

* To whom correspondence should be addressed. Present address: Bionic Design Group, National Institute for Advanced Interdisciplinary Research (NAIR), MITI, 1-1-4 Higashi, Tsukuba, Ibaraki 305, Japan. Phone: +81-298-54-2557. Fax: +81- 298-54-2565.

[⊗] Abstract published in *Advance ACS Abstracts,* December 1, 1995.

(1) Elliott, J. C. *Structures and Chemistry of the Apatites and Other Calcium Orthophosphates*; Elsevier Science Publishers B. V.: Amsterdam, 1994; Studies in Inorganic Chemistry, Vol. 18.
(2) Kanazawa, T. *Inorganic phosphate materials*; Kodansha Tokyo and Elsevier Science Publishers B. V.: Amsterdam, 1989; Materials science monographs, Vol. 52.
(3) Posner, A. S. *Clin. Orthop.* **1985**, *200*, 87.
(4) Legeros, R. Z. *Calcium phosphates in oral biology and medicine*; Karger, Basel, 1991; Monographs in Oral Science, Vol. 15.
(5) De Groot, K. *Bioceramics of calcium phosphate*; CRC Press: Boca Raton, FL, 1983.
(6) Jarcho, M. *Clin. Orthop. Rel. Res.* **1981**, *157*, 259.
(7) Hench, L. L. *J. Am. Ceram. Soc.* **1991**, *74*, 1511.
(8) Brendel, T.; Engel, C.; Russel, C. *J. Mater. Sci.: Mater. Med.* **1992**, *3*, 175.
(9) Fauchais, P.; Vardelle, A.; Vardelle, M. *Ceram. Int.* **1991**, *17*, 367.
(10) (a) Kay, M. I.; Young, R. A.; Posner, A. S. *Nature* **1964**, *204*, 1050. (b) $Ca_{10}(PO_4)_6(OH)_2$: JSPDS 9-432 ($a = 9.418$ Å; $c = 6.884$ Å).
(11) (a) Sudarsanan, K.; Mackie, P. E.; Young, R. A. *Mater. Res. Bull.* **1972**, *7*, 1331. (b) $Ca_{10}(PO_4)_6F_2$: JSPDS 15-876 ($a = 9.368$ Å; $c = 6.884$ Å).
(12) Sudarsanan, K.; Young, R. A. *Acta Crystallogr.* **1978**, *B34*, 1401.
(13) Moreno, E. C.; Kresak, M.; Zahradnik, R. T. *Nature* **1974**, *247*, 64.
(14) Moreno, E. C.; Kresak, M.; Zahradnik, R. T. *Caries Res.* **1977**, *11 (Suppl.1)*, 142.
(15) Okazaki, M.; Aoba, T.; Doi, Y.; Takahashi, J.; Moriwaki *J. Dent. Res.* **1981**, *60*, 845.
(16) Okazaki, M. *Biomaterials* **1992**, *13*, 749.
(17) Freund, F.; Knobel, R. M. *J. Chem. Soc., Dalton Trans.* **1977**, 1136.
(18) (a) Young, R. A.; Van der Lugt, W.; Elliott, J. C. *Nature* **1969**, *223*, 729. (b) Van der Lugt, W.; Knottnerus, D. I. M.; Perdok, W. *Acta Crystallogr.* **1971**, *B27*, 1509. (c) Braun, M.; Hartmann, P.; Jana, C. *J. Mater. Sci.: Mater. Med.* **1995**, *6*, 150.
(19) Prener, J. S. *J. Electrochem. Soc.: Solid State Sci.* **1967**, *114*, 77.
(20) Kanazawa, T.; Monma, H.; Enomoto, S.; Nunozawa, M. *J. Ceram. Soc. Jpn.* **1977**, *85*, 96.

0897-4756/96/2808-0134$12.00/0

by the action of β-$Ca_3(PO_4)_2$ on CaF_2 through a solid-state reaction at about 1200 °C in a N_2 gas flow (F found 3.72 wt %, $x = 0.99$).[20] Nevertheless, pure fluoroapatite can not be obtained by direct precipitation in an aqueous basic $Ca^{2+}-PO_4^{3-}-F^-$ system even if high fluorine concentrations are used.[14−16] Effectively, the resulting precipitates are usually contaminated by small amount of HO^- replacing F^- in the channels of the apatitic structure. Therefore, this ionic competition between HO^- and F^- during the precipitation in water allows only the formation of a FHAP material with a maximum fluorine content of 3.58 wt % and $x = 0.95$.[14−16]

Moreover, several studies have shown that in the presence of high concentrations of calcium and phosphorus, a transient phase named amorphous calcium phosphate [ACP] precipitates in water.[22] As the mineral part of calcified tissues presents a poor crystallinity, the formation of the amorphous precursor and its transformation into the hydroxyapatite phase have been thoroughly investigated in vitro.[23−29] In water slurries and under specific chemical conditions (i.e., high temperature, low supersaturation, and ionic strength, neutral pH) the metastable ACP phase can be converted into stable crystalline HAP by a process of dissolution and renucleation in a few hours.[28,29] This transformation is water-mediated, and certain investigations have shown that the presence of nonaqueous solvents (i.e., ethanol, acetone) barely delayed the conversion.[23] Indeed, during previous work, we have directly precipitated an amorphous octacalcium phosphate [OCP; Ca/P = 1.33] from calcium and phosphate water/ethanol (50/50) alkaline solutions.[30] Partially aqueous solvents with lower dielectric constants hardly decrease the solubility of calcium phosphates. By rapid mixing, high supersaturations are attained instantaneously, kinetic factors may favor and stabilize the ACP metastable precipitate instead of the thermodynamic crystalline HAP phase. However, fluorine may be associated with formation of apatitic calcium phosphate, as a reaction and crystallization accelerator in its initial stage.[16,31] Effectively, the conversion of amorphous into apatitic calcium phosphate in aqueous suspension proceeds more rapidly when fluorine ions are present.[31]

Naturally, synthetic amorphous calcium phosphate has been studied by conventional and more advanced techniques.[32−38] The ACP material has been characterized by the absence of peaks in its X-ray diffraction pattern (XRD),[22] by a loss of resolution in ν_3 and ν_4 PO_4 vibration bands in comparison with the normally degenerate infrared absorption spectra of apatites,[32] and by spherical particles with diameter 30−100 nm without structure in their electron micrographs.[33] Using radial distribution function (RDF) from X-ray data, Betts and Posner proposed a "structural" model of ACP.[34] This is composed of roughly spherical elementary clusters, 0.95 nm in diameter, of $Ca_9(PO_4)_6$ in which the Ca^{2+} and PO_4^{3-} ions positions are approximately the same as those in hydroxyapatite. However, HO^- ions, which are located inside tunnels of the HAP lattice, are absent in this spherical model focused on the Ca atom (type I) coordinates.[35] Recently, extended X-ray absorption fine structure (EXAFS) studies on the Ca K absorption edge have shown that only three shells of atoms surrounding a Ca^{2+} were necessary to fit with the ACP spectra instead of the nine shells required for fully crystalline HAP.[36] These three shells, with a radius of 0.35 nm, which corresponded to the two oxygen and one phosphorus, resemble the radii in the HAP model; however, they are more disordered. It has been concluded that the transformation of ACP into poorly crystalline HAP proceeds without any change in the local environment of Ca, but simply involves an increase in long-range order in the structure.[36]

For these reasons, it would be interesting to prepare by a soft chemistry process stoichiometric FAP in a nonaqueous media in the presence of fluorine ions. Recently, we discovered a new synthesis method, producing calcium phosphates in pure ethanol from $Ca(OEt)_2$ and H_3PO_4.[37] The organometallic calcium source $Ca(OEt)_2$ is completely soluble in ethanol and liberates the conjugate base of the solvent EtO^-. This strong base neutralizes H_3PO_4. Following reaction 1, an amorphous

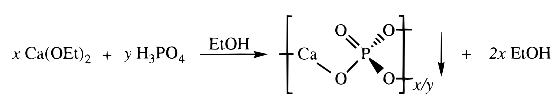

(1)

and nanosized calcium phosphate gelatinous precipitate is obtained during this neutralization, and the sole byproduct is ethanol. However, our first study focused on the precipitation in anhydrous ethanol of calcium phosphates with a maximum Ca/P ratio of 1.50 ($x = 9$ and $y = 6$ in eq 1).[37a]

In this work, calcium phosphate materials with Ca/P ratios close to 1.66 are precipitated with and without fluorine ions in a nonaqueous media. The resulting amorphous solids are characterized by conventional physicochemical analyses and X-ray photoelectron spectroscopy (XPS). Their thermal behaviors are also studied to ensure their chemical and microstructural homogeneities. Finally, a mechanism of formation of these mineral compounds in this pure organic medium is proposed.

Experimental Section

Materials. Calcium metal shavings (99%) and anhydrous orthophosphoric acid crystals (98+%) were purchased from Aldrich. Ammonium fluoride (analytical grade) and anhydrous

(21) Maiti, G. C. *Indian J. Chem.* **1990**, *29A*, 402.
(22) Eanes, E. D.; Gillensen, I. H.; Posner, A. S. *Nature* **1965**, *208*, 365.
(23) Termine, J. D.; Peckauskas, R. A.; Posner, A. S. *Arch. Biochem. Biophys.* **1970**, *140*, 318.
(24) Bosquey, A. L.; Posner, A. S. *J. Phys. Chem.* **1973**, *77*, 2313.
(25) Eanes, E. D.; Meyer, J. L. *Calcif. Tiss. Res.* **1977**, *23*, 259.
(26) Meyer, J. L.; Eanes, E. D. *Calcif. Tiss. Res.* **1978**, *25*, 59.
(27) Meyer, J. L.; Weatherall, C. C. *J. Colloid. Interface Sci.* **1982**, 89, 257.
(28) Tung, M. S.; Brown, W. E. *Calcif. Tissue Int.* **1983**, *35*, 783.
(29) M. R. Christoffersen; J. Christoffersen; W. Kibalczyc *J. Cryst. Growth* **1990**, *106*, 349.
(30) Lebugle, A.; Zahidi, E.; Bonel, G. *Reactivity Solids* **1986**, *2*, 151.
(31) Meyer, J. L.; Nancollas, G. H. *J. Dent. Res.* **1972**, *51*, 1443.
(32) Termine, J. D.; Lundy, D. R. *Calcif. Tiss. Res.* **1974**, *15*, 55.
(33) Eanes, E. D.; Termine, J. D.; Nylen, M. U. *Calcif. Tissue Res.* **1973**, *12*, 143.
(34) Betts, F.; Posner, A. S. *Mater. Res. Bull.*. **1974**, *9*, 353.
(35) Betts, F.; Posner, A. S. *Trans. Am. Cryst. Assoc.* **1974**, *10*, 73.
(36) Harries, J. E.; Hukins, D. W. L.; Holt, C.; Hasnain, S. S. *J. Cryst. Growth* **1987**, *84*, 563−70.
(37) (a) Layrolle, P.; Lebugle, A. *Chem. Mater.* **1994**, *11*, 1996. (b) Layrolle, P. Thèse de l'INP, Toulouse, France, 1994.
(38) (a) Pascal, P. *Nouveau Traité de Chimie Minérale: Azote, Phosphore, Tome X*; Masson and Cie: Paris, 1956; p 159. (b) *Handbook of Chemistry and Physics*, 64th ed.; CRC Press: Boca Raton, FL, 1984, p B68. (c) *The Merck Index*, 9th ed.; Merck & Co. Inc.: Rahway, NJ, 1976; p 72.

Table 1. Synthesis Conditions of Samples Obtained by Mixing $Ca(OEt)_2$, H_3PO_4, and NH_4F Reagents in Anhydrous Ethanol at 80 °C

procedures/ samples	SOL A[a]	SOL B[b]		Ca/P liquid (molar ratio)
	Ca metal (g)	H_3PO_4 (g)	NH_4F (g)	
CP	1.332	1.960		1.66
CPF	1.287	1.896	0.409	1.67
CF	1.910		3.580	

[a] +50 mL of EtOH. [b] +200 mL of EtOH.

ethanol were commercially obtained from Prolabo. These materials were used without further purification and all other materials for chemical characterizations were Prolabo analytical grade. The synthesis was performed under a dry atmosphere with vacuum/argon manifolds for air-sensitive products. Conventional glassware was used.

Sample Preparation. The different solids were obtained in pure ethanol starting from $Ca(OEt)_2-H_3PO_4-NH_4F$ reagents in two solutions named **SOL A** and **SOL B**. The quantities of reagents in these two solutions were given in the Table 1. The procedures used for the preparation of samples are shown schematically in Figure 1 and described below.

*Preparation of **SOL A***. The calcium diethoxide $Ca(OEt)_2$ solution was prepared by reacting calcium metal with ethanol, as previously published.[37] Briefly, the appropriate amount of calcium metal and ethanol were put under argon gas in a round-bottom flask equipped with a condenser. The solution was refluxed for 4 h until all the metallic calcium disappeared.

*Preparation of **SOL B***. According to Table 1, the second solution contained NH_4F and/or H_3PO_4 reagents and was prepared as follow. The quantity of NH_4F was solubilized with constant stirring under argon gas in 200 mL of ethanol in a 500-mL flask equipped with a condenser. The decomposition of NH_4F with heating provided hydrofluoric acid and ammonia gas according to the reaction 2. As HF is more soluble than NH_3, the reaction produced soluble fluorine ions in ethanol.[38] This HF solution was used in the precipitation of samples **CF** or **CPF**.

$$NH_4F \rightarrow NH_3\uparrow + HF\uparrow \qquad (2)$$

To precipitate sample **CP**, an exact stoichiometric quantity of H_3PO_4 crystals for an initial liquid Ca/P molar ratio of 1.66 was dissolved by stirring and heating at 80 °C in ethanol. In a separate reaction, the calculated amount of anhydrous H_3PO_4 for a Ca/P = 1.66 was added to the previously described fluorine ethanolic solution to prepare sample **CPF**.

Mixing, Gel Precipitation, Separation, and Drying. When **SOL A** was added quickly through a cannula to the vigorously stirred **SOL B** at 80 °C, a white gelatinous precipitate formed immediately. The gel precipitate was maintained under reflux, stirring, and argon for 2 h to complete the reaction. After cooling to room temperature, the gelatinous precipitate was centrifuged and the supernatant was removed. Then, the resulting wet solids were dried under vacuum at room temperature overnight. Finally, the fine white powder was crushed, put into a shlenk flask under argon and stored at −20 °C in a refrigerator to prevent hydrolysis and crystallization.

Chemical Analyses. The powdered samples (100 mg) were dissolved in 5 mL of $HClO_4$ (2 M), and the solution was diluted to 100 mL in a volumetric flask with deionized water. Calcium was titrated by a complexometric method using an EDTA disodium salt in the presence of zinc chloride with eriochrome black T as an indicator.[39] The relative error on calcium determination was ±1%. The orthophosphate content was determined by a spectrometric measurement of the phosphovanadomolybdate yellow complex using a Beckman Model 24 spectrophotometer at a wavelength of 460 nm.[40] Relative error

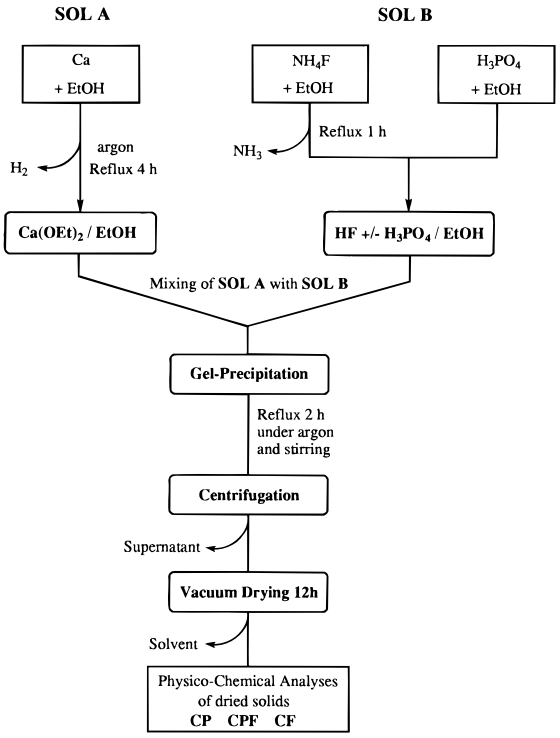

Figure 1. Flowchart of the ethanol synthesis process of calcium phosphate **CP** and **CPF** and calcium fluoride **CF** solids according to three different experimental procedures.

on replicates was ±1%. The calcium to phosphorus atomic ratios (Ca/P) were found to correspond to the ratios expected from the starting materials to within ±0.02. Fluorine concentration was determined by potentiometry with a specific ion and a calomel reference electrodes.[41] The relative error on fluorine determination was ±2%. The amount of carbonate was measured with a UIC Coulometrics Model 5010 coulometer. Carbonate content was assayed with a relative error of ±1%. Microanalyses C, H, N were obtained with a Carlo-Erba Model 1106 elemental analyzer. The relative errors on determination of these elements were respectively 0.3, 0.1, and 0.3%.

Infrared Spectroscopy. Infrared absorption spectra (IR) were recorded on a Perkin-Elmer FT-IR 1600 spectrometer using transparent KBr pellets: 1−2 mg of the sample was crushed and mixed with 300 mg of KBr (Prolabo, spectroscopic grade). The powder was pressed at 14 tons cm^{-2} under vacuum (∼1 Torr) in a 13 mm cylinder mold for 10 min to obtain a transparent disk. Absorbance FT-IR spectra shown are the result of coding 16 scans obtained over the 4000−400-cm^{-1} region with a resolution of 2 cm^{-1}.

X-ray Powder Diffraction. The XRD patterns of the samples were obtained at room temperature with a Sigma 2060 generator operated at 45 kV and 28 mA using a cobalt source and a quartz monochromator selecting the Co Kα wavelength (λ = 1.788 92 Å). The XRD patterns were recorded for 1 h using an Inel X-ray CPS 120 curved position-sensitive detector for simultaneous measurement of several diffracted lines. Hexagonal lattice parameters a_0 and c_0 were determined on 300, 310, 410 and 002, 004 reflections, respectively. For the precise determination of d_{hkl} values, α-Al_2O_3 (30 wt %) was used as an internal standard (JSPDS 10−173). Deviations in d_{hkl} positions did not exceed ±0.005 Å.

X-ray Photoelectron Spectroscopy. The XPS spectra were performed by using an Escalab Mk II spectrometer, with an Al Kα X-ray source (14866 eV of photon energy). The powdered samples were examined on Scotch tape. The power source was limited to 300 W. The survey spectra were recorded with a constant analyzer pass energy of 50 eV and step size of 0.5 eV. The regional spectra were obtained with

(39) Charlot, G. *Les Méthodes de la Chimie Analytique, Analyse Quantitative et Minérale*, 5th ed.; Masson and Cie: Paris, 1966; p 657.
(40) Gee, A.; Deitz, V. R. *Anal. Chem.* **1953**, *25*, 1320.
(41) Duff, E. J.; Stuart, J. L. *Anal. Chim. Acta* **1970**, *52*, 155.

Table 2. Chemical Analyses of Vacuum-Dried Solids Prepared in Pure Ethanol

	chemical analyses (wt %)							Ca/P
samples	Ca[a]	PO_4[b]	F[c]	CO_3[d]	C[e]	H[e]	N[e]	solid (molar)
CP	32.6	46.3		4.8	3.2	0.8	1.67	1.67
CPF	32.9	46.7	4.5		2.1	1.1	0.6	1.67
CF	50.9		48.3		⩽0.1	⩽0.1	0.2	

[a] Calcium content was determined by the complexometric method. [b] Orthophosphate was assayed by the vanadomolybdate spectrophotometric method. [c] Fluoride content was measured by the potentiometric method using a specific ion electrode. [d] Carbonates were assayed by a Coulometric method after conversion to CO_2 gas. [e] Carbon, hydrogen, and nitrogen microanalyses included the contribution of several compounds: trapped ethanol, carbonate, adsorbed water, hydrogen phosphate, and ammonium.

a constant analyzer energy fixed at 20 eV and a step size of 0.1 eV. The positions of the peaks, altered by the electric charge accumulated by the insulating sample, were corrected by referencing to aliphatic carbon C_{1s} (E_b = 285.0 eV). The accuracy on the binding energy was ±0.1 eV. Single crystals were also used as reference materials: a stoichiometric FAP obtained by the Czochralski method at 1650 °C under pure argon[42] and a mineral CaF_2 crystal provided by the Mineralogy Laboratory of the Paul Sabatier University, Toulouse (France). The intensities of the P_{2p}, Ca_{2p}, O_{1s}, and F_{1s} peaks were integrated with Lorentzian and Gaussian functions using the VG building software and the Scofield relative cross section.[43] From these peaks areas, a quantitative evaluation of the XPS data was performed and formulas were calculated. In the case of calcium phosphates, the Ca/P ratio was refined by using a multiplying factor of 1.12 determined for pure HAP.[44]

Thermal Analyses. Thermogravimetric and differential thermal analyses (TGA, DTA) were carried out in a Setaram TG-DTA 92 thermobalance provided with a data acquisition and processing system. About 20 mg of the sample was placed in cylindrical alumina crucibles 5 mm in diameter and 10 mm in height. A U-grade helium constant flow of 1 L h^{-1} at atmospheric pressure was employed. α-Al_2O_3 was used as the reference material for DTA measurements. Temperatures were measured with Pt/Rh thermocouples located at the bottom of the alumina crucibles. A linear heating rate of 10 °C min^{-1} was monitored over in the 20−1000 °C temperature range.

Thermal Treatment. The samples were placed in a platinum boat, into a quartz tube, and inside a laboratory tubular furnace. The solids were heated from room temperature to successively 500, 700, and 900 °C in N_2 at a ramp rate of 100 °C h^{-1}. Each sample was held at the final temperature for 2 h, allowed to cool rapidly to room temperature, and then examined by several analytical techniques.

Scanning Electron Microscopy. SEM observations were performed on a Jeol JSM-6400 instrument. The samples were ultrasonically dispersed in anhydrous ethanol. Then, the suspension was deposed in a carbon support, dried under vacuum and coated with a fine layer of Ag to reduce charging effects.

Results and Discussion

The procedures used for the preparation of the different samples are shown schematically in Figure 1. As previously described, the different solids were obtained using $Ca(OEt)_2$, H_3PO_4, and NH_4F by mixing two solutions in anhydrous ethanol. In **SOL A**, the soluble and highly basic calcium source $Ca(OEt)_2$ can neutralize H_3PO_4 and/or HF in **SOL B**. During this spontaneous neutralization, a gelatinous precipitate was formed. In the procedure **CPF**, the initial reagents were simultaneously introduced with a stoichiometry close to that of a FAP compound (see Table 1). To understand the mechanism of formation of the sample **CPF**, two other solids named **CP** and **CF** were precipitated following the same experimental conditions but modifying the stoichiometries of the reagents. Thus, only $Ca(OEt)_2$ and H_3PO_4 were used to prepare a calcium phosphate solid in the route named **CP**. In the last procedure, **CF**, $Ca(OEt)_2$, and NH_4F were mixed to synthesize fluorine CaF_2 in ethanol. Then, the three resulting solids were characterized by the following physicochemical analyses.

Chemical Analyses. In Table 2, chemical analyses (Ca, PO_4, F, CO_3, C, H, N) of the vacuum dried solids **CP**, **CPF**, and **CF** are given. These results show that sample **CP** contained calcium, orthophosphate, and carbonate ions. As the precipitation process was completed under argon and no source of carbonate was introduced, the presence of CO_3^{2-} anions in sample **CP** is unexpected and will be discussed later. In contrast, solid **CPF** did not contain carbonate ions, only calcium, phosphate, and fluorine ions were present. Molar Ca/P ratios calculated from chemical analyses for calcium phosphate samples **CP** and **CPF** equaled 1.67. These values are very close to the molar Ca/P ratios of the initial reagents in solution ($[Ca/P]_L$ = 1.66).

Only three possibilities can account for the presence of fluorine ions in the calcium phosphate fluorine precipitate **CPF**:

(1) The fluorine could be associated with ammonium ions, resulting from the fluorine source employed here, to form an insoluble NH_4F salt trapped in the final solid.

Since the nitrogen content of sample **CPF** was very low (0.6 wt %, 0.043 mol), this hypothesis can be easily rejected. The dried precipitate **CPF** included very little NH_4^+ (calcd: 0.8 wt %). The F^- content is too high (4.5 wt %, 0.237 mol) to be completely associated with NH_4^+. So, the majority of fluorine ions are included in this calcium phosphate precipitate **CPF** in another form than NH_4F.

(2) Fluorine anions could be offset with calcium cations to precipitate fluorine CaF_2 in approximately the same time as a calcium phosphate precipitate. The resulting solid should be composed of *two different mineral compounds* such as $Ca_9(PO_4)_6$ and CaF_2.

(3) Fluorine could be included in *a single calcium phosphate fluoride precipitate* with chemical and structural arrangement close to that of a FAP, $Ca_{10}(PO_4)_6F_2$, compound.

These two possibilities, referring, respectively, to the formation of two different or a single mineral compound(s), will be intensively discussed throughout this paper.

Chemical analyses of solid **CF** precipitated in ethanol with $Ca(OEt)_2$ and NH_4F reagents show that calcium and fluorine were major elements. Only traces of nitrogen (0.2 wt %) resulting from NH_4^+ were detected by microanalyses. It was noticed that weight percentages were very close to those in calcium fluorine CaF_2 (theor wt %: Ca: 51.28, F: 48.72). The **CF** synthesis procedure can undoubtedly form an insoluble CaF_2 compound following eq 3.

(42) Heughebaert, J. C.; Seriot, J.; Joukoff, B.; Gaume-Mahn, F.; Montel, G. *C. R. Acad. Sc. Paris*, **1975**, *281 Ser. C*, 615.
(43) Scofield, J. H. *J. Electron Spectrosc.* **1976**, *8*, 129.
(44) (a) Lebugle, A.; Sallek, B. *Hydroxyapatite and Related Materials;* Brown, P. W., Constantz, B., Eds.; CRC Press: Boca Raton, FL, 1994; p 319. (b) Lebugle, A.; Rovira, A.; Rabaud, M.; Rey, C. *J. Mater. Sci.: Mater. Med.*, submitted.

$$Ca(OEt)_2 + 2HF \rightarrow CaF_2\downarrow + 2EtOH \qquad (3)$$

Infrared Spectroscopy. FT-IR absorbance spectra of solids **CP** and **CPF** are shown in Figure 2. These two FT-IR spectra present large and poorly defined bands that can be identified by their extremums or shoulders. Both spectra show the vibrations of tetrahedral PO_4 groups.[42] In the **CP** spectrum, vibrations assigned to carbonate ions were observed.[45] In solid **CPF**, ammonium ions were also detected by the weak band at 1400 cm^{-1}. This very low NH_4^+ content was already assayed by C, H, N microanalyses (Table 2), and it is due to the NH_4F reagent employed in the **CPF** processing. Thus, trace amounts of ammonium are trapped in the final solid **CPF**. In addition, both spectra show large and strong bands due to large amounts of ethanol and/or water trapped in these calcium phosphate precipitates.

PO_4 and HPO_4 Bands. Both spectra show the strong ν_3 and ν_4 P−O vibrations of PO_4 groups situated respectively near 1050 and 565 cm^{-1}.[45] However, a lack of resolution in these PO_4 bands is observed. These one-component, broad, highly symmetric and featureless phosphate absorption bands suggest that these two calcium phosphate solids prepared in ethanol are amorphous. Indeed, the phosphate ions in these amorphous solids are not subjected to the regular distortions due to constraints from the crystal lattice (as in the case of apatites).[32] On the contrary, these spectra are quite similar to that from perfect tetrahedral phosphate ions in solution.[46] Nevertheless, by careful examination of the PO_4 vibrations in the spectra of **CP** and **CPF**, a shoulder at about 950 cm^{-1} for the symmetric stretch ν_1 mode can be seen. As this ν_1 (A_1) mode is IR inactive in the undistorted and free tetrahedral PO_4^{3-} ions, a lower symmetry is obviously required (i.e., group symmetry C_{3v}).[47] This local lower symmetry can be easily explained if slight differences in the P−O lengths and/or O−P−O dihedral angles are present in these amorphous calcium phosphate solids. It is probable that calcium ions strongly attached by Coulombian forces to the PO_4 groups induce the distortions of the tetrahedrons. Effectively, the ν_1 shoulders observed in both FT-IR spectra could be the result from a preferential bond between calcium and orthophosphate ions (i.e., one oxygen of one PO_4^{3-} linked with a Ca^{2+}), resulting in the establishment of a local short-range order in the solid state. Certainly, it would be interesting to confirm these observations by Raman spectroscopy that is very sensitive to P−O vibrations, in particular, to the ν_1 mode.

In the spectrum **CPF**, the very weak and broad vibration at 875 cm^{-1} is undoubtedly assigned to P−O(H) stretch of some HPO_4^{2-} ions (no CO_3 bands in the 1500−1430 cm^{-1} region). These hydrogen phosphate bands are the cause of hydrofluoric acid produced on heating the **SOL B** (see eq 2). Thus, more acidic conditions are present during precipitation of the **CPF** solid. However, regarding the very low absorbance intensities of these bands, a trace amount of HPO_4^{2-} ions is present in solid **CPF** which is mainly composed of PO_4^{3-} ions.

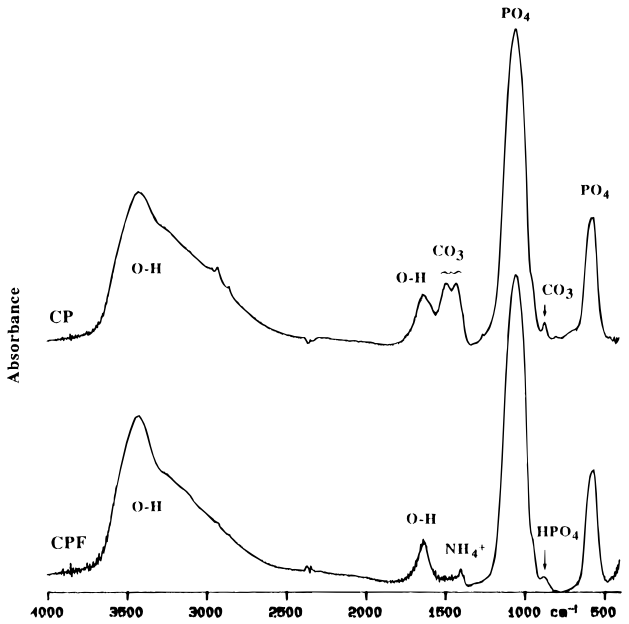

Figure 2. FT-IR absorbance spectra of calcium phosphate vacuum-dried solids **CP** and **CPF** recorded from 4000 to 400 cm^{-1} (KBr pellets).

CO_3 Bands. By comparing the two FT-IR spectra, several additional bands due to CO_3^{2-} ions were observed in the solid **CP** precipitated without fluoride ions. The two peaks situated near 1490 and 1426 cm^{-1} are assigned to the ν_3 vibration mode and the very weak vibration at about 870 cm^{-1} is due to the ν_2 mode of free, planar CO_3^{2-} ions (group symmetry D_{3h}).[45,47] However, these features of the CO_3 bands in the spectra of the carbonated calcium phosphate solid **CP** are different from the vibrations normally observed in calcite, $CaCO_3$: Specifically, the ν_4 vibration mode at about 710 cm^{-1} is absent and the ν_3 asymmetric stretch for the undistorted CO_3^{2-} ions near 1500 cm^{-1} is split into two components. These differences of CO_3 bands in the spectrum of the sample **CP** with those of well-known calcite suggest that the CO_3^{2-} ions are in a disordered environment. The features observed in the FT-IR spectrum of the carbonated calcium phosphate solid **CP** are due to slight differences in the C−O lengths. Thus, the CO_3^{2-} ions in sample **CP** have lower symmetries than D_{3h}.

EtOH and H_2O Bands. In the two spectra, broad and strong bands at about 3425 and 1630 cm^{-1} are assigned to O−H stretching and bending of hydrogen-bonded EtOH and/or H_2O molecules. Shoulders at about 2900 cm^{-1} due to C−H stretching of the EtOH groups are also visible. These vibrations suggest that ethanol and possibly water are trapped and/or adsorbed in these two calcium phosphate solids during their synthesis processes, their crushing and characterization in air.

X-ray Diffraction. The XRD patterns of the three samples precipitated in pure ethanol following the procedures **CP**, **CPF**, and **CF** are presented in Figure 3.

Solid **CF** was fully crystallized, and the positions and intensities of its X-ray diffraction peaks were in total accordance with those given in the literature for the cubic cell CaF_2 (JSPDS 35−816). The lattice constant a_0 found was equal to 5.461 Å and was very close to the

(45) Nakamoto, K. *Infrared Spectra of Inorganic and Coordination Compounds*; John Wiley & Sons, Inc.: New York, 1963.
(46) Steele, D. *Theory of vibrational spectroscopy*; W. B. Saunders Co.: Philadelphia, 1971.
(47) Chapman, A. C.; Thirlwell, L. E. *Spectrochim. Acta* **1964**, *20*, 937.

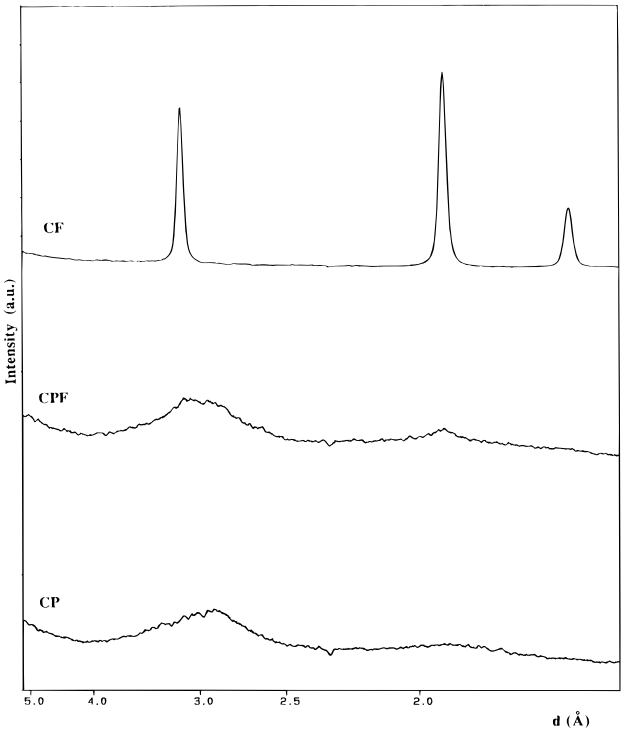

Figure 3. XRD patterns of the different solids **CP**, **CPF**, and **CF** precipitated in ethanol and dried under vacuum overnight.

theoretical value, $a_0 = 5.4626$ Å. Moreover, no other phases, such as starting NH_4F, were detected by XRD. This is in agreement with the chemical analyses described above. Therefore, when the **CF** synthesis procedure is used, CaF_2 with high purity and crystallinity is precipitated in ethanol according to reaction 3.

In contrast, samples **CP** and **CPF** were characterized by the absence of peaks in their XRD patterns. Their diagrams show only diffuse halos whose maximums were located at about 3.0 and 1.8 Å. These two "bumps" are usually observed in the pattern of amorphous calcium phosphate precipitated in water and they are also coinciding with apatite major lines.[10,11,22] Thus, the solids **CP** and **CPF** are amorphous to X-ray diffraction confirming the previous observations made by FT-IR. Even though chemical analyses show a carbonate content of 4.8 wt % for sample **CP** (see Table 2), no peaks of crystalline $CaCO_3$ were detected in its diffractogram. In the same manner, the composition of solid **CPF** indicated a fluoride content of 4.5 wt %, but in its XRD pattern we did not observe the peaks expected for crystalline CaF_2 or NH_4F. As the **CF** synthesis procedure allows the precipitation of a well-crystallized calcium fluoride powder and not an amorphous one, the noncrystalline sample **CPF** prepared in the same condition could be a unique, homogeneous, and well-defined calcium phosphate fluoride compound, in agreement with the above third hypothesis. However, this solid **CPF** could be composed of two insoluble compounds consistent with the second hypothesis. In this case, crystalline CaF_2 should be highly microdispersed in the final calcium phosphate material so that it forms crystals too small to be observed by XRD. To settle this question, these solids were studied by XPS spectroscopy that give information on the chemical arrangement of the different atoms Ca, P, O, and F independent of crystallinity. Their thermal behavior was also studied

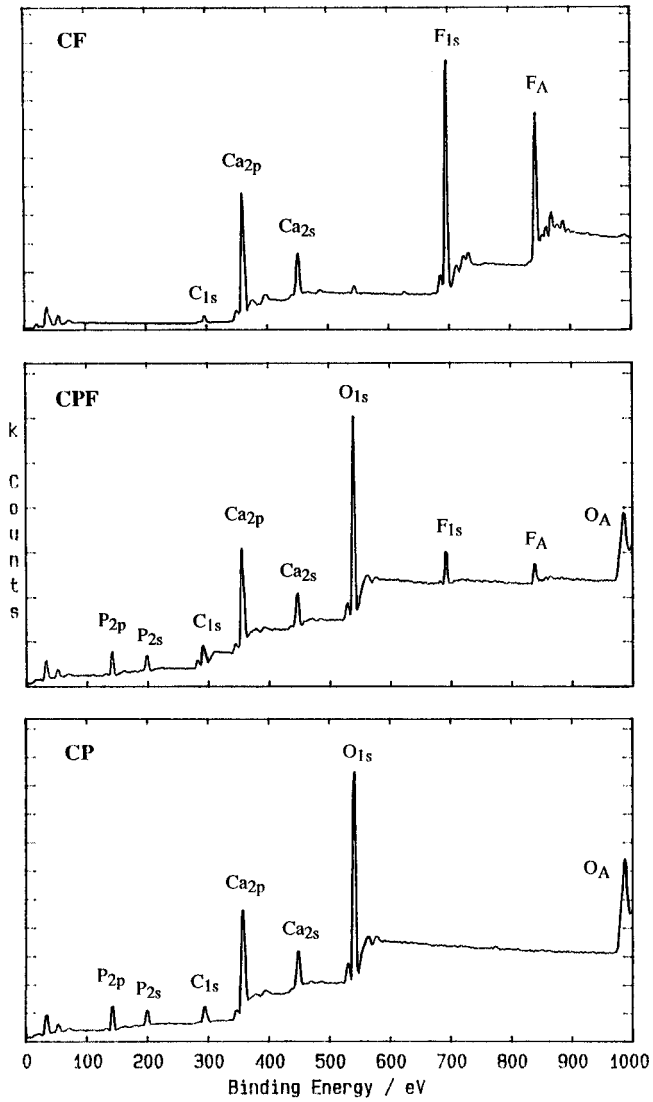

Figure 4. XPS survey spectra of the precipitates **CP**, **CPF**, and **CF**.

by several techniques to ensure their chemical and structural homogeneities.

X-ray Photoelectron Spectroscopy. The survey spectra of the solids **CP**, **CPF**, and **CF** are shown on Figure 4. The main constituents of the samples, calcium, phosphorus, oxygen, or fluorine, can easily be seen through their photoelectronic peaks. In all the spectra, excess carbon is observed due to contamination (scotch tape). This C_{1s} peak at 285.0 eV was used as an internal reference to correct the positions of the XPS peaks. Thus, the region spectra of P_{2p}, Ca_{2p}, O_{1s}, and F_{1s} allowed the binding energies and the full width at half height [$\omega_{1/2}$] to be measured with accuracy (±0.1 eV). The corresponding values are gathered in Table 3. The positions of the peaks were compared with those reported for HAP[44] and with those of FAP and CaF_2 single crystals.

In each of the solids studied, the $Ca_{2p_{3/2}}$ and F_{1s} regional peaks are both strictly symmetric. In contrast, in the amorphous **CP** or **CPF** samples, O_{1s} peaks are asymmetric and they can be decomposed into two components (see Table 3). The main component sited at lower energy was assigned to an oxygen linked to one phosphorus atom and corresponds to the PO_4^{3-} ions. The binding energy of the second component at 533.6 eV is

Table 3. Positions and Full Width at Half-Height [$\omega_{1/2}$] of XPS of the Different Solids Compared with Those of Standards

samples standards	XPS peaks positions[a] and [$w_{1/2}$] (eV)				
	P_{2p}	$Ca_{2p^{3/2}}$	$O_{1s}(1)$	$O_{1s}(2)$	F_{1s}
CP	133.6 [2.50]	347.8 [2.50]	531.6 [2.47] 90%	533.5 [2.69] 10%	
CPF	133.7 [2.53]	347.8 [2.39]	531.7 [2.35] 82%	533.6 [2.20] 18%	685.0 [2.47]
CF		348.6 [2.33]			685.5 [2.19]
HAP[b]	133.6 [2.34]	347.6 [2.42]	531.5 [2.25]		
FAP[c]	133.6 [2.12]	347.7 [1.94]	531.6 [1.96]		684.7 [1.83]
CaF_2[c]		348.6 [1.70]			685.5 [1.70]

[a] Positions were corrected using C_{1s} peak at 285.0 eV. The precision on the peak positions was ±0.1 eV. [b] From ref 44. [c] Single crystals.

close to the one observed in compounds where the oxygen atom is linked to two atoms of lower electronegativities, such as P−O−H, H−O−H and R−O−H (R being aliphatic).[44] Thus, the XPS analyses confirm the presence of adsorbed water and/or trapped ethanol in these amorphous solids.

In the XPS spectra of the two noncrystalline calcium phosphates **CP** and **CPF**, the binding energies of $Ca_{2p_{3/2}}$ and P_{2p} have the same values and equal 347.8 and 133.7 eV, respectively. Moreover, these positions correspond to those given in literature for calcium phosphate apatites.[44] In the amorphous sample **CPF**, the binding energies of $Ca_{2p_{3/2}}$, P_{2p}, and F_{1s} are also in agreement with the value measured for the fluoroapatite single crystal. However, these peaks exhibit a larger $\omega_{1/2}$ than is observed for the crystalline FAP standard due to the amorphous state of the solid **CPF**. In the sample **CF**, the binding energies of $Ca_{2p_{3/2}}$ and F_{1s} equal 348.5 and 685 eV, respectively, corresponding to those observed in the CaF_2 single crystal. In addition, it is important to emphasize that both of these values are higher than those observed in fluoroapatite. This can be explained by considering that CaF_2 and FAP have not the same crystalline potential . It is well-known that the binding energy of elements is depending on the crystalline potential in which the atoms are sited, as shown by the following relation:

$$Eb = Eb_0 + k_iQ_i + Er_i + V_{i,j}$$

where Eb_0 is the atomic binding energy, k_i a constant, Q_i the partial atomic charge on atom i, Er_i the relaxation energy, and $V_{i,j}$ the crystalline potential. In ionocovalent compounds, the relaxation energy can be neglected. Thus, it is possible to calculate the crystalline potential of calcium and fluorine ions in each lattice, by using a computer program developed by Piken.[48] The charges of calcium, phosphorus, oxygen, and fluoride ions were equal to +2.00, 1.60, −1.15, and −1.00, respectively, according to a previous study.[49] The positions of atoms used were the same as those indicated in literature.[11]

As far as the calcium atom is concerned, its crystalline potential is equal to −18.9 eV in the FAP structure (average between the values obtained for calcium located in sites of types I and II) and it is equal to −19.9 eV in the CaF_2 lattice. Thus, the crystalline potential for calcium ions is more negative in the fluorine than in the FAP structure. Consequently, it would be more difficult to extract an electron from these atoms and the binding energy of the Ca_{2p} peak is higher in CaF_2 than in FAP, as experimentally observed. Furthermore, the computed shift of 1.0 eV is close to the value observed of 0.9 eV. In the same manner, the crystalline potential of fluoride is equal to +11.2 eV in FAP and to +10.7 eV in CaF_2. As the potential is less positive in the second structural unit, an electron sited on an F atom would be hardly extracted by the X-ray radiation, and its binding energy would be higher in CaF_2 than in FAP, in agreement with the experimental results. Besides, the computed and observed shifts are the same (0.5 eV). Due to these different binding energies, the XPS analysis could easily distinguish a small amount of CaF_2 in the sample **CPF** whatever its crystallinity.

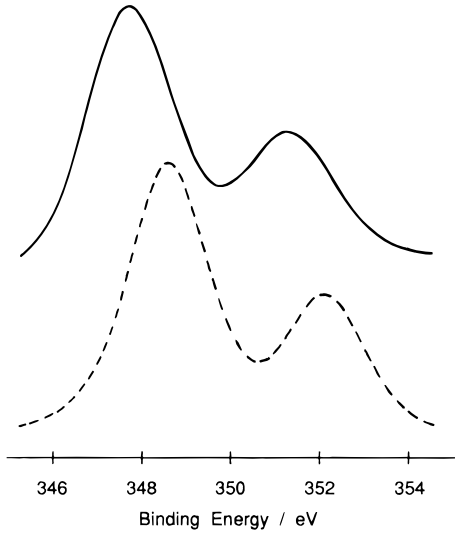

Figure 5. XPS regional spectrum for the Ca_{2p} peaks of solids **CF** (dotted line) and **CPF** (solid line).

The expanded Ca_{2p} and F_{1s} peaks of the samples **CPF** and **CF** are compared on Figures 5 and 6. The two peaks observed on Figure 5 corresponds to the two atomic levels $Ca_{2p_{3/2}}$ and $Ca_{2p_{1/2}}$. As the two precipitates obtained in ethanol exhibit very different XPS peaks positions, it can be deduced that there is no CaF_2 embedded as a separate phase in the amorphous solid **CPF**. Indeed, if the material contained CaF_2, the $Ca_{2p_{3/2}}$, and F_{1s} peaks would not be symmetric. Therefore, the amorphous solid **CPF** is certainly a single and homogeneous material according to the previous third hypothesis.

In addition, the quantitative analysis of the noncrystalline precipitate **CPF** was performed from integrated peak intensities with Scofield's relative cross sections by using calcium apatite and fluorine as standards to take into account matrix effects. Formula and atomic ratios were calculated and reported in Table 4 along

(48) Piken, A. G.; Van Gool, W. *Computer Program for Calculations of Electrostatic Self-Potentials Madelung Constants and Energy of Ionic Componds*; Ford Motor Co., 1968.
(49) Devarajan, V.; Klee, W. E. *Phys. Chem. Miner.* **1981**, *7*, 35.

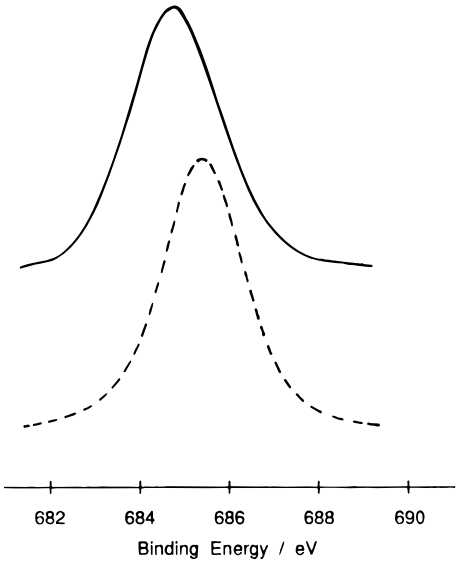

Figure 6. XPS regional spectrum for the F_{1s} peaks of solids **CF** (dotted line) and **CPF** (solid line).

Table 4. Comparison of Atomic Ratios and Raw Formula Determined by XPS and Chemical Analyses of CPF

analyses	Ca/P	O(1)/P	O(2)/P	F/P	formula
XPS	1.70	3.90	0.85	0.50	$Ca_{1.7}PO_{3.9}F_{0.5}$· 0.85(H_2O, EtOH)
chemical	1.67			0.48	$Ca_{1.67}PO_4F_{0.48}$· x(H_2O, EtOH)

with those drawn from chemical analysis. It appears that the Ca/P ratio determined by the half-quantitative XPS analysis is in good agreement with the value assayed. The O(1)/P ratio is very close to 4 and so corresponds to a PO_4 group. The O(2)/P ratio allows us to conclude that there are 0.85 of water and/or residual ethanol. These molecules are adsorbed onto the amorphous **CPF** solid by strong links that are not broken even under high vacuum in the XPS spectrometer. Effectively, it has been well established that amorphous or poorly crystallized calcium phosphates precipitated in aqueous slurries frequently retain about 10−20 wt % of water. It has been shown that water is strongly attached to these solids and cannot be removed by drying at room temperature.[46] Thus, water and/or ethanol could surely play a role in the stabilization of the amorphous state. In addition, the raw formula calculated from XPS and chemical analyses were also in a good agreement. These formulas correspond to a fluoridated calcium phosphate material which has the same chemical composition of a FAP compound.

Thermal Behavior. The thermogravimetric analyses for vacuum dried solids **CP**, **CPF**, and **CF** are shown in Figure 7. The sample **CF**, that was previously identified by chemical analysis and by XRD as CaF_2, shows a TGA profile very different from the other. The total weight loss was below 2.5%, and two very little steps can be seen in its TGA curve. The first weight loss of 0.9% situated near 80 °C and the second of 1.2% situated from 230 to 320 °C were attributed to the removal of the residual solvent and the decomposition of trace NH_4F. For both calcium phosphates **CP** and **CPF**, single and continuous weight losses of respectively 13.1% and 8.6%, were observed in approximately the same temperature range 100−400 °C. These weight losses can be principally assigned to the evaporation/

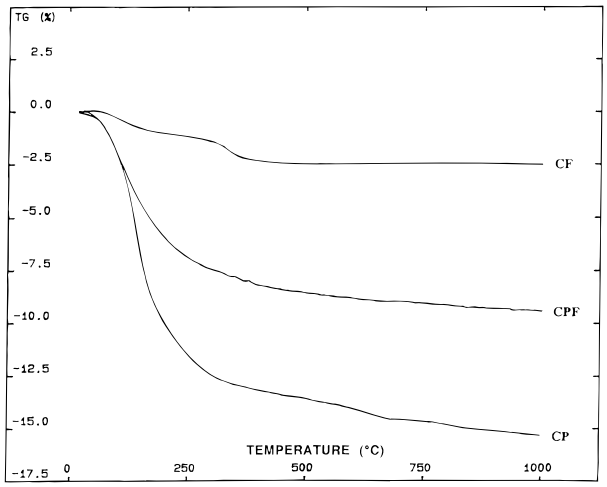

Figure 7. TG analyses under helium flow of the different powders **CF** (m_0 = 38.26 mg), **CP** (13.69), and **CPF** (14.32) in the range 20−1000 °C (heating rate 10 °C min^{-1}).

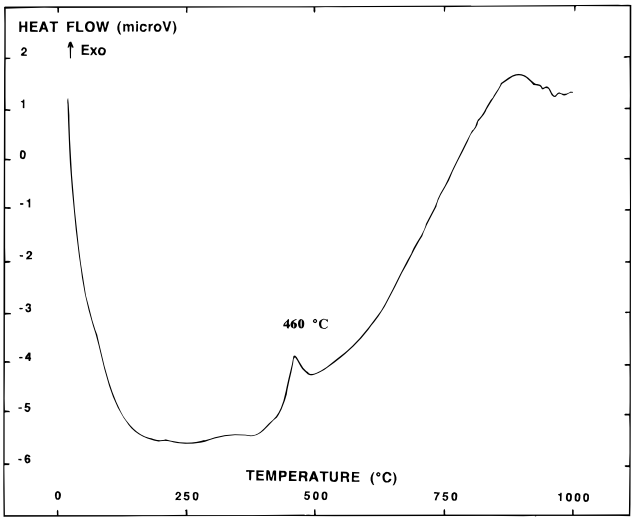

Figure 8. DTA curve of the calcium phosphate sample **CPF** (simultaneous measurement from TGA).

desorption of ethanol and water trapped or adsorbed in these amorphous solids. According to the TG analyses, all the solvent was eliminated in the solids at 500 °C and the ceramic yield was about 80%. In addition, TGA curve of sample **CP** shows a weight loss equal to about 2.9% spreading in the range 400−970 °C with a visible, small step near 650 °C. Between these temperatures, carbonate ions contained in sample **CP** were progressively transformed to CO_2 gas resulting in the observed continuous weight loss.

Simultaneous differential thermal analysis (DTA) profiles were recorded for the three samples. Only the DTA curve of solid **CPF** is shown in Figure 8 because of its interesting exothermic peak at 460 °C, just before the large and intense endothermic drift due to the corresponding weight loss in TGA. For the two other samples **CP** and **CF**, the DTA profiles did not show exothermic peaks in the range 20−1000 °C. Only a large endothermic drift from 50 to 500 °C with a maximum at about 150 °C due to the evaporation/desorption of ethanol and water was observed in the DTA of sample **CP**. In Figure 8, the exothermic signal, linearly integrated from 420 to 488 °C gave a negative enthalpy of −29.2 mJ mg^{-1}. This exothermic peak could be assigned to the thermal crystallization of amorphous

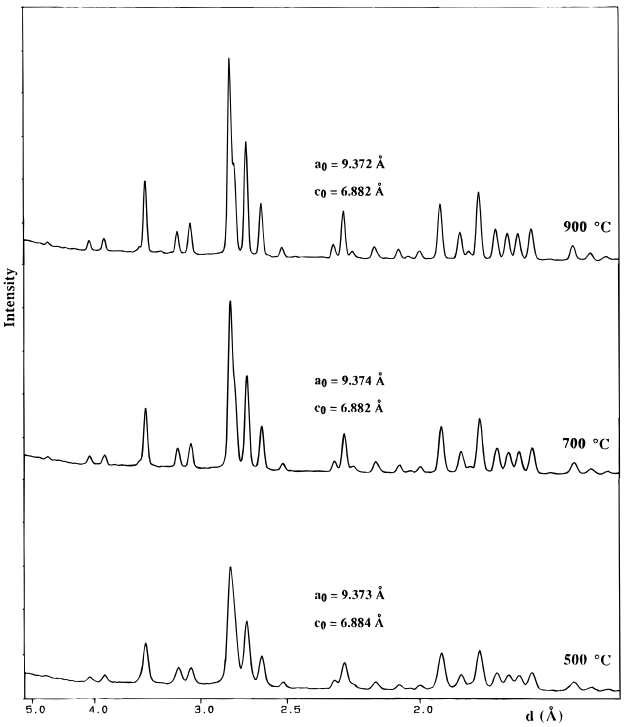

Figure 9. XRD patterns and calculated lattice parameters of sample **CPF** heated to 500, 700, and 900 °C in N_2.

solid **CPF** into a crystalline fluoroapatite compound in agreement with the previous third hypothesis. This analysis further confirms the absence of CaF_2 in the material, as a single exothermic peak at 460 °C is observed. If CaF_2 was present, an endothermic peak around 800 °C (may be just before two distinct exothermic peaks of crystallization) would be seen due to a solid state reaction between CaF_2 and β-$Ca_3(PO_4)_2$ leading to a FAP compound. Therefore, this single exothermic peak of crystallization proves the chemical and structural homogeneities of the initial amorphous sample **CPF**.

Figure 9 shows the XRD patterns of solid **CPF** heated from room to different temperatures in N_2. Up to 400 °C, sample **CPF** remain amorphous, but after heating to 500 °C, it is evidently crystallized. This is in agreement with the temperature of crystallization previously observed by DTA. It has been shown that the thermal crystallization of amorphous calcium phosphate into β-$Ca_3(PO_4)_2$ phase begins at approximately 700 °C.[50] It is surprising that here the crystallization of the amorphous sample **CPF** occurs at a lower temperature. The positions and intensities of diffraction lines were in total accordance with those of a hexagonal apatitic lattice. Increasing the heating temperature to 700 and to 900 °C led to more sharp and narrow diffraction peaks resulting from an improved crystallinity. Additional transient phases, even as traces, such as crystalline CaF_2 or β-$Ca_3(PO_4)_2$ were never detected by XRD during heating of solid **CPF** and only the fluoroapatite phase was observed. This point favors the hypothesis that **CPF** is a single and homogeneous material. Calculated lattice constants a_0 and c_0 of heated samples are reported in Figure 9. These cell parameters were very close to those given in the literature for a stoichiometric

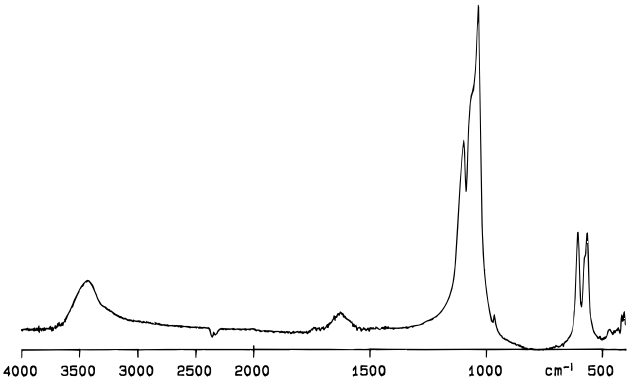

Figure 10. FT-IR absorbance spectrum of solid **CPF** heated to 500 °C in N_2.

fluoroapatite.[11] If a solid solution FHAP was formed, an intermediate value for a_0 parameter should be observed between those of FAP and HAP.[10,11] Therefore, a pure FAP has crystallized by heating to 500 °C the amorphous precipitate **CPF**. The heated solids were also studied by FT-IR spectroscopy to confirm the previous XRD observations. The spectrum of sample **CPF** heated to 500 °C is shown in Figure 10. Indeed, it is well established that −O−H−F− channel stretching and bending bands can be observed in the 3540 and 745 cm^{-1} region, even if slight amount of hydroxide ions is incorporated in the lattice of a FHAP solid solution.[17] In our heated samples, these bands were never observed and the FT-IR spectra were characteristic of a stoichiometric FAP from 500 °C (see Figure 10). On the other hand, bands previously assigned to adsorbed ethanol or water were not present in the FT-IR spectra of solid heated to 500 °C. These volatile compounds were eliminated at this temperature confirming the TGA curve (see Figure 7). Therefore, XRD and FT-IR spectroscopy studies have shown that a pure FAP can be easily prepared by our synthesis method. The use of a nonaqueous solvent avoids the ionic competition between hydroxide and fluorine ions.[14−16] In addition, if we compare our method to the solid-state preparations of the stoichiometric FAP,[19−21] an important energetic saving is obtained by our soft chemistry process.

In Figure 11, the SEM micrographs of the precipitates **CP**, **CPF**, and **CF** are shown. For both amorphous calcium phosphates **CP** and **CPF** approximately the same morphology was observed by electron microscopy: strongly agglomerated spherical particles with diameters in the range 50−100 nm. These nanosized particles do not have preferential orientations, and their spherical morphology and size are very similar of those of amorphous precipitates obtained at high supersaturation in water.[33] The centrifugation process and the high surface areas are responsible for agglomerates of several microns in size. Cubic or needles resulting from microcrystalline $CaCO_3$, CaF_2, or an apatitic phase embedded in these amorphous solids **CP** and **CPF** were never observed even at high magnification. It would be interesting to confirm these results by high-resolution electron transmission microscopy (HREM) which is better adapted to distinguish or detect other phase in amorphous calcium phosphate materials.[51] On the other hand, the SEM micrograph of the crystalline solid

(50) Kanazawa, T.; Umegaki, T.; Uchiyama N. *J. Chem. Tech. Biotechnol.* **1982**, *32*, 399.

(51) Bres, E. F.; Moebus, G.; Kleebe, H.-J.; Pourroy, G.; Werkmann, J.; Ehret, G. *J. Cryst. Growth* **1993**, *129*, 149.

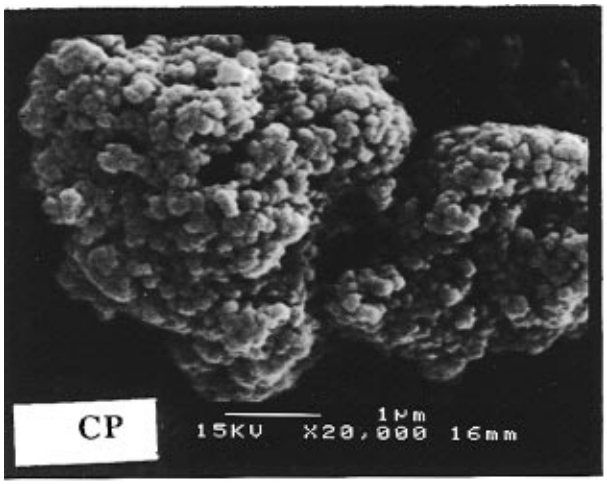

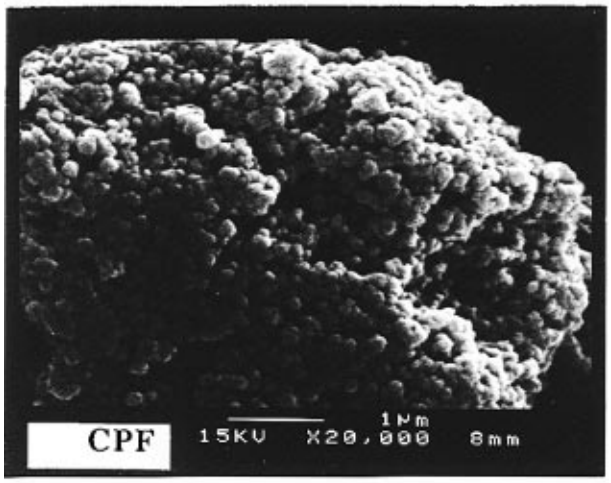

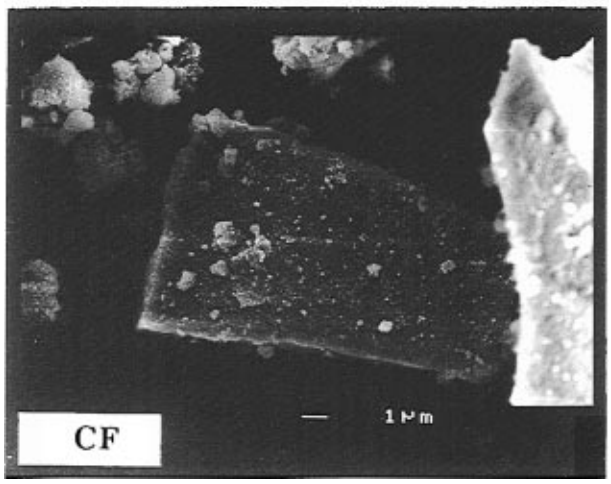

Figure 11. SEM micrographs of as-prepared solids **CP**, **CPF** and **CF**.

CF, assigned to CaF_2, shows a completely different morphology. The sizes and morphologies of the crystalline precipitate **CF** differ considerably from the two amorphous calcium phosphates **CP** and **CPF**. The polycrystalline powder obtained in ethanol presents large faces and square edges of cubic crystals of CaF_2.

A SEM micrograph of the sample **CPF** heated to 500 °C is shown in Figure 12. Joints and necks between the initial nanosized spherical particles are clearly visible in the micrographs of the heated solid. The finely divided material obtained in ethanol after heating

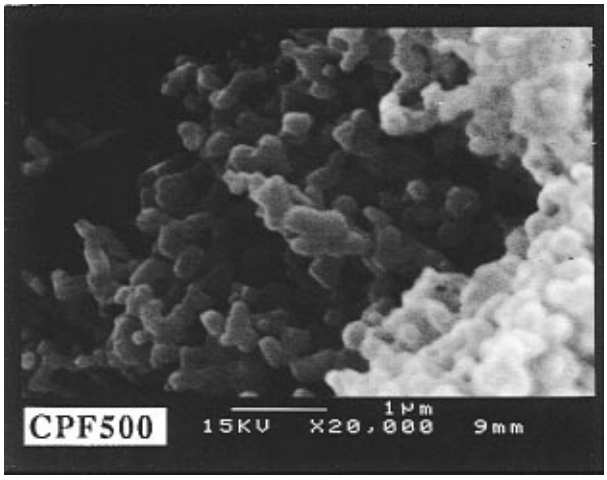

Figure 12. SEM micrographs of (CPF500) amorphous sample **CPF** heated to 500 °C in N_2.

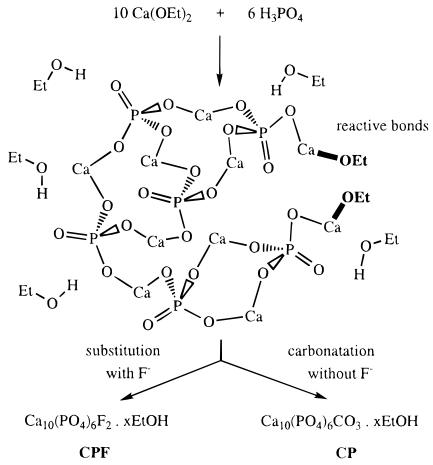

Figure 13. Mechanism of formation of the amorphous solid **CPF** and **CP** precipitated in ethanol with or without the fluoride source added in **SOL B**.

to 500 °C showed a strong grain growth due to its high reactivity. This low-temperature diffusion process associated with the crystallization of vacuum-dried amorphous samples was already observed in our previous work.[37a] The high reactivity of the amorphous solid **CPF** precipitated in ethanol could be used for the preparation of FAP ceramics at very low temperature. This type of soft chemistry synthesis has advantages over the conventional sintering process of crystalline powder. Indeed, rare-earth-doped FAP ceramics are often used for laser applications due to their excellent luminescent properties.[2] In our soft chemistry method, doped FAP ceramics could be easily obtained at several hundred degrees lower than in the other high temperature routes.

Reaction Pathways and Mechanism. From several physicochemical analyses employed here, a mechanism of formation of these mineral compounds in a pure organic medium is proposed on Figure 13. When the starting ethanolic solutions of $Ca(OEt)_2$ and H_3PO_4 are mixed rapidly in a stoichiometry 10/6, precipitation of a calcium phosphate gel occurs spontaneously. Unlike the other sol−gel processes,[52] addition of water for the polycondensation is not necessary here. Indeed, the

(52) Brinker, C. J.; Scherrer, G. *Sol-Gel science, The physics and chemistry of Sol−Gel processing*; Academic Press: New York, 1990.

neutralization of orthophosphoric acid by the very basic organometallic calcium reagent leads to an intermediate calcium phosphate solid with the same Ca/P molar ratio of the starting. As shown in Figure 13, these mineral aggregates are likely surrounded by ethanol molecules strongly linked by hydrogen and donor interactions. Resulting from this adsorption, the solvent can not be removed under vacuum at room temperature but only after heating to 500 °C (Figure 7). However, as these nanosized materials have large surface areas, they are highly reactive to moisture. Thus, the ethanol adsorbed on these amorphous solids could be progressively replaced by water which has a stronger dielectric constant.

The presence of CO_3^{2-} ions in solid **CF** can be explained as follow. Without fluorine ions added to the **SOL B**, pendant alkoxy groups remains attached to calcium in the gelatinous precipitate obtained under argon. Refluxing this solid in ethanol did not cause any segregation that could give a mixture of a solid calcium phosphate with a Ca/P ratio equal to 1.50 and a soluble $Ca(OEt)_2$ precursor. After centrifugation and drying, the calcium phosphate **CP** solid formed had a Ca/P ratio closed to 1.66. However, during its characterization, the very reactive and basic EtO^- groups bonded to calcium spontaneously reacted with moisture and carbon dioxide contained in air to lead carbonate ions. Indeed, we have previously observed a similar carbonation of the very sensitive $Ca(OEt)_2$ solid in contact with air.[37b] In the same way, CO_2 gas bubbling in the **SOL A** also produced an insoluble and amorphous $CaCO_3$ mineral compound in anhydrous ethanol.[37b] Therefore, the final carbonated calcium phosphate **CP** observed here is certainly the result of the same decomposition in air of the ethoxy groups.

In the presence of fluorine ions in **SOL B** but without the phosphate source (procedure **CF**), the carbonation did not occurred but a rapid substitution of EtO^- by F^- was observed producing an insoluble and fully crystalline CaF_2 mineral compound according to reaction 3.

In the procedure **CPF**, where fluorine and phosphorus ions were simultaneously introduced in **SOL B**, the same substitution occurred, leading to an amorphous fluoridated calcium phosphate solid **CPF**. Moreover, this gelatinous solid was not in final chemically and structurally heterogeneous (e.g., mixed crystalline CaF_2 and ACP phases) even if it was kept in refluxed ethanol for 2 h. The amorphous **CPF** solid has the same chemical composition as that of a pure FAP compound (see Table 4). A wide-angle X-ray scattering study has already been employed to propose a structural model for the first amorphous fluoridated calcium phosphate that has a Ca/P ratio of 1.66 (to be published).

Conclusions

A new synthesis route in pure ethanol, using $Ca(OEt)_2$, H_3PO_4, and NH_4F reagents, enables the formation of an amorphous and nanosized fluoridated calcium phosphate **CPF** solid with a Ca/P of 1.66. Moreover, it has the same chemical composition as a fluoroapatite compound. The amorphous state of the **CPF** solid is probably stabilized by some ethanol molecules strongly adsorbed into the mineral aggregates. Besides, XPS spectroscopy shows that the P_{2p}, Ca_{2p}, O_{1s}, and F_{1s} peaks have the same binding energies as those in a FAP material. These atoms in the amorphous solid **CPF** should have a local chemical and structural arrangements similar to a FAP phase but lacking long-range order. Indeed, this material is not composed of two amorphous phases, such as $Ca_9(PO_4)_6$ and CaF_2. As the synthesis is done in an anhydrous solvent, the amorphous **CPF** precipitate heated to 500 °C in N_2 crystallize into an exactly pure fluoroapatite (without hydroxyl ions in its structure). In addition, no foreign phases such as CaF_2 and/or β-$Ca_3(PO_4)_2$ were ever detected by XRD before or after its crystallization. In the same way, only a single exothermic signal at 460 °C was observed on the DTA curve. This confirms the homogeneity of the amorphous **CPF** phase precipitated in ethanol. After heating the nanosized **CPF** powder to 500 °C, a very active sintering is observed by SEM. This is due to the high reactivity of our material synthesized by this soft chemistry process.

Acknowledgment. This work was supported by a Ph.D. Research Grant number 160-INP-91 to the Ministère de l'Enseignement Supérieur et de la Recherche of France. We grateful acknowledge Professor Christian Rey for his helpful discussions and suggestions in IR spectroscopy. The authors wish to thank Gérard Dechambre for his collaboration in reproducing some figures. We are indebted to Professor Jean-Claude Heughebaert for giving the fluoroapatite single crystals.

CM950326K